Temperature-controlled release by changes to the secondary structure of peptides anchored on mesoporous silica supports

Cristina de la Torre, Alessandro Agostini, Laura Mondragón, Mar Orzaez, Félix Sancenón, Ramón Martinez-Máñez, Enrique Pérez-Payá and Pedro Amorós

Chemicals

The chemicals tetraethylorthosilicate (TEOS), *n*-cetyltrmethylammonium bromide (CTABr), sodium hydroxide (NaOH), safranine O, diisopropylethylamine (DIEA), 4-pentynoic acid, anhydrous dimethylformamide (DMF), trifluoroacetic acid (TFA), 2,2,2-trifluoroethanol (TFE), triisobutylsilane (TIS) and sodium ascorbate were purchased from Sigma-Aldrich Química (Madrid, Spain) and used without further purification. Copper (II) sulfate pentahydrate ($CuSO_4 \cdot 5H_2O$) was purchased from Scharlab (Barcelona, Spain). HPLC grade amino acids and resin TG SRAM were purchased from Iris Biotech. Oxyma pure, azidopropyltriethoxysilane, tripyrrolidinophosphonium hexafluorophosphate (PyBOP) and HPLC grade solvents were obtained from Merck (Barcelona, Spain).

General techniques

PXRD, TG Analysis, elemental analysis, EDX microscopy, N_2 adsorption-desorption were employed to characterize the prepared materials. Power X-ray measurements were performed on a Philips D8 Advance diffractometers using Cu K_α radiation. Thermogravimetric analysis were carried out on a TGA/SDTA 851e Mettler Toledo balance, using an oxidant atmosphere (air, 80 ml/min) with a heating program consisting on a heating ramp of 10 ºC per minute from 393 to 1273 K and an isothermal heating step at this temperature during 30 minutes. Fluorescence spectroscopy was carried out on a Felix 32 Analysis Version 1.2 PTI (Photon Techonology International). TEM images were obtained with a 100 kV Philips CM10 microscope. Peptides were synthesized employing an automatic peptide synthesizer 422A from Applied Biosystems. Purification and analysis of the complete peptide sequence by HPLC were carried out by means of a Merck Hitachi L-2130 HPLC pump and a sample carrier L-2200 with a Lichospher 100 C18 (250x10 mm) column. The eluent was monitored at 220 nm employing a Merck Hitachi UV Detector L-2200 autosampler and employing a Licrhsopher 100 C18 (150x3.9 mm) column, and as mobile phase different acetonitrile-aqueous TFA (0.1%) mixtures. Mass spectrometry analysis was performed employing a MALDI TOF/TOF 4700 Proteomics Analyzer from Applied Biosystems. Circular dichroism measurements were carried out in a JASCO 810.

Synthesis of peptide sequence (P)

Peptide sequence H-SAAEAYAKRIAEALAKG-OH was synthesized by Fmoc-based solid phase chemistry using a 433A Applied Biosystem Peptide Synthesizer. Once, the complete sequence of the peptide was obtained, 4-pentynoic acid was added to the sequence at the *N*-terminal side through an amide bond using PyBOP, DIEA and oxyma pure. The peptide was cleaved from the resin by treatment with trifluoroacetinc acid (TFA 94%, TIS 1% and H_2O 5%) during 4 hours and purified by preparative RP-HPLC (Lycrospher 100 C18, 10 mm) using acetonitrile-aqueous TFA (0.1%) mixtures. The identity and purity was confirmed by HPLC and MALDI-TOF mass spectrometry.

Synthesis of mesoporous silica nanoparticles

The MCM-41 mesoporous nanoparticles were synthesized by the following procedure: *n*-cetylmethylammonium bromide (CTABr, 1.00 g, 2.74 mmol) was first dissolved in 480 ml of deionized water. Then a 3.5 ml of NaOH 2.00 M in deionized water was added to the CTABr solution, followed by adjusting the solution temperature to 80 ºC. TEOS (5.00 ml, 2.57 x 10^{-2} mol) was then added dropwise to the surfactant solution. The mixture was allowed to stir for 2h to give a white precipitate. Finally the solid product was centrifuged, washed with deionized water and ethanol, and was dried at 60 ºC (MCM-41 as-synthesized). To prepare the final porous material (MCM-41), the as-synthesized solid was calcined at 550 ºC using oxidant atmosphere for 5 h in order to remove the template phase.

Synthesis of solid S1

Calcined MCM-41 (500 mg) and safranine O (140 mg, 0.4 mmol) were suspended in acetonitrile (15 mL). Then the suspension was stirred for 24 hours at room temperature with the aim of achieving the maximum loading in the pores of the MCM-41 scaffolding. Afterward an excess of 3-(azidopropyl)triethoxysilane (0.62 g, 2.5 mmoles) was added, and the suspension was stirred for 5.5 h. Finally, the solid was filtered off and dried at vacuum.

Synthesis of solid S1-P

For the preparation of the solid **S1-P**, azide-functionalized nanoparticles **S1** (30 mg) and the peptide **P** (30 mg) were suspended in a 50:50 v/v DMF-H_2O mixture (30 ml) in the presence of an excess of safranine O (200 mg, 0.8 mmol) in order to avoid the delivery of the dye from the pores to the bulk solution during the synthesis of the final solid. Then, 100 μL of a solution of $CuSO_4 \cdot 5H_2O$ (10^{-3} mol dm^{-3}) and 100 μL of sodium ascorbate (10^{-2} mol dm^{-3}) were added. The reaction mixture was stirred at 90 ºC for 3 days. The nanoparticles were centrifuged and washed thoroughly with water to remove unreacted and absorbed molecules. The resulting red nanoparticles were finally dried under vacuum.

Materials characterization

Solid **S1** was characterized using standard procedures. Figure SI-1 shows powder X-ray patterns of the nanoparticulated MCM-41 support and the **S1** functionalised material. The PXRD of siliceous nanoparticulated MCM-41 as-synthesized shows four low-angle reflections typical of a hexagonal array that can be indexed as (100), (110), (200) and (210) Bragg peaks. A significant displacement of the (100) peak in the PXRD powder of the nanoparticulated MCM-41 calcined sample is clearly appreciated in curve b, corresponding to an approximate cell contraction of 4 Å. This displacement and the broadening of the (110) and (200) peaks are related to further condensation of the silanol groups during the calcinations step. Curve c corresponds to the **S1** PXRD pattern. In this case, a slight intensity decrease and the disappearance of the (110) and (200) reflections were observed, most likely related to a loss of contrast due to the filling of the pore voids with the safranine O. Nevertheless, the value and intensity of the (100) peak in this pattern strongly evidences that the loading process with the dye and the further functionalization with 3-(azidopropyl) triethoxysilane have not damaged the mesoporous 3D MCM-41 scaffolding. The curve d corresponds to the **S1-P** PXRD pattern.

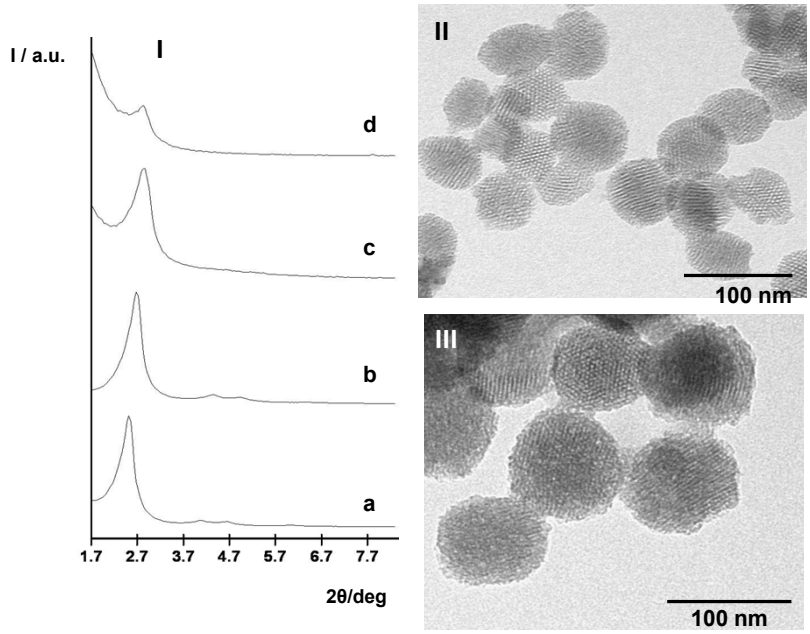

Figure SI-1. (I) Power X-ray diffraction patterns of the solids (a) MCM-41 as-synthesized, (b) calcined MCM-41 , (c) solid **S1** containing safranine O dye and 3-(azidopropyl)triethoxysilane and (d) solid **S1-P** containing safranine O dye and the peptide **P**. TEM images of MCM-41 calcined (II) and final solid **S1-P** (III).

Preservation of the mesoporous structure in the final functionalized solids was also confirmed by means of TEM. Figure SI-1 shows the morphology of the MSN materials. As it can be seen, the MCM-41 material was obtained as spherical particles with diameters of ca. 80 nm, and the loaded and functionalized derivative **S1-P** keep the initial morphology of the MCM-41 matrix. The figure also shows the typical channels of the MCM-41 matrix either as alternate black and white stripes or as a pseudohexagonal array of pore voids. These channels are visualized not only in the calcined material but also in **S1-P**.

Further DLS (Dynamic Light Scattering) studies showed particles with a mean diameter of 75.92 nm for MCM-41 and of 89.01 nm for **S1-P** materials (see Table SI-1). The differences in the nanoparticle diameter could be ascribed to the surface functionalization with the bulky 17-mer peptide **P**. Also, Figure SI-2 showed that calcined MCM-41 nanoparticles and the final material **S1-P** formed aggregates of 271.35 and 545.07 nm of diameter, respectively. However, only about 4% of the total nanoparticles are in the aggregated state (see also Table SI-1).

Table SI-1. Diameter of MCM-41 calcined and **S1-P** nanoparticles.

	Diameter (nm)	% of nanoparticles
MCM-41	75.92	96.75
	271.35	3.25
S1-P	89.01	96.13
	545.07	3.87

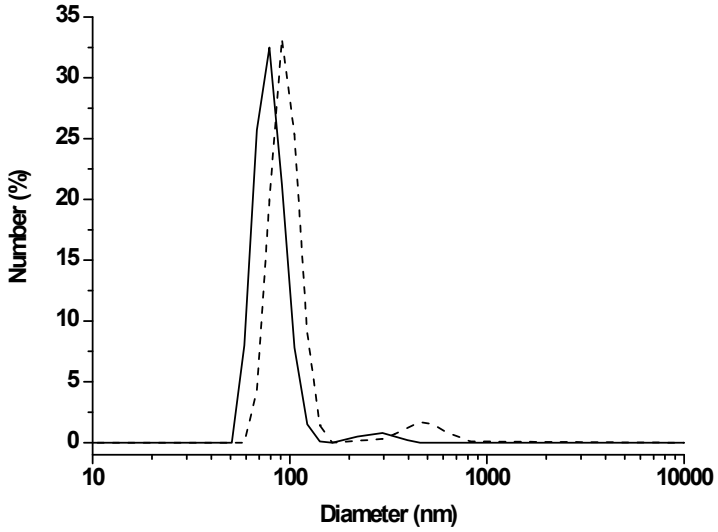

Figure SI-2. Size distribution by number of particles obtained by DLS studies. The average size of nanoparticles of calcined MCM-41 (straight), **S1-P** (dash) was found to be ca. 90-100 nm.

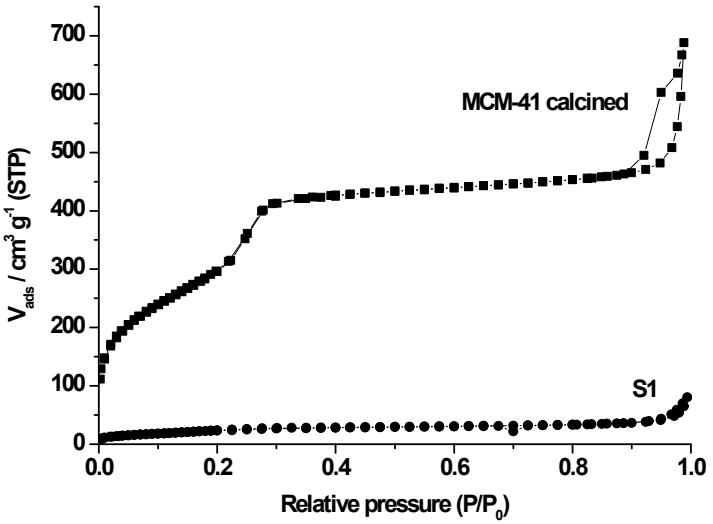

Figure SI-3. Nitrogen adsorption-desorption isotherms for MCM-41 mesoporous material and **S1**.

The N_2 adsorption-desorption isotherms of the nanoparticulated MCM-41 calcined material shows an adsorption step at intermediate P/P_0 value (0.1-0.3) typical of this solids (see Figure SI-3). This step can be related to the nitrogen condensation inside the mesopores by capillarity. The absence of a hysteresis loop in this interval and the narrow BJH pore distribution suggest the existence of uniform cylindrical mesopores. The application of the BET model resulted in a value for the total specific surface of 1096.5 m^2/g and a pore volume of 0.78 cm^3/g. From the PXRD, porosimetry and TEM studies, the a_0 cell parameter (4.43 nm), the pore diameter (2.45 nm) and the value for the wall thickness (1.98 nm) were calculated. In addition to this adsorption step associated to the micelle generated mesopores, a second feature appears in the isotherm at a high relative pressure. This adsorption correspond to the filling of the large void among the particles, present a volume of 0.24 g/cm (calculating by using the BJH model) and

must be considered as a textural-like porosity. In this case, the curves show a characteristic H1 hysteresis loop and a wide pore size distribution.

The N_2 adsorption-desorption isotherm of **S1** is typical of mesoporous systems with filled mesopores, and a significant decrease in the N_2 volume adsorbed and in the specific surface area (90.7 m^2/g) is observed (see Figure SI-3). In fact, this solid shows flat curves when compared (at the same scale) to those of the MCM-41 parent material, this indicates a significant pore blocking and the subsequent absence of appreciate mesoporosity. Additionally, a certain textural porosity is preserved. BET specific surface values, pore volumes and pore sizes calculated from the N_2 adsorption-desorption isotherms for MCM-41 and **S1** are listed in Table SI-2.

Table SI-2. BET specific surface values, pore volumes and pore sizes calculated from the N_2 adsorption-desorption isotherms for selected materials.

	S_{BET} ($m^2\ g^{-1}$)	Total pore volume ($cm^3\ g^{-1}$)	BHJ pore (nm)
MCM-41	1096.5	0.78	2.45
S1	90.7	0.06	-

The content of 3-(azidopropyl)triethoxysilane, safranine O and peptide in **S1** and **S1-P** solids were determined by elemental and thermogravimetric analysis. Values of contents are detailed in table SI-3.

Table SI-3. Content in mmol of anchored molecules and dye in mmol g^{-1} SiO_2 for solids **S1** and **S1-P**.

	Azide (mmol g^{-1} SiO_2)	Safranine O (mmol g^{-1} SiO_2)	Peptide (mmol g^{-1} SiO_2)
S1	0.246	0.544	-
S1-P	0.246	0.250	0.041

Dye delivery studies

To investigate the temperature-responsive gating properties of **S1-P**, 4 mg of solid were suspended in 5.5 ml of water and then fractioned into seven parts of 500 μL. The seven fractions were stirred at different temperatures (4, 17, 25, 30, 37.5, 60 and 90 ºC). After 3 hours of stirring the delivery of safranine O from the seven samples was determined through the measurement of their emission band centered at 580 nm (upon excitation at 520 nm). The release kinetic curve is shown in Figure SI-4.

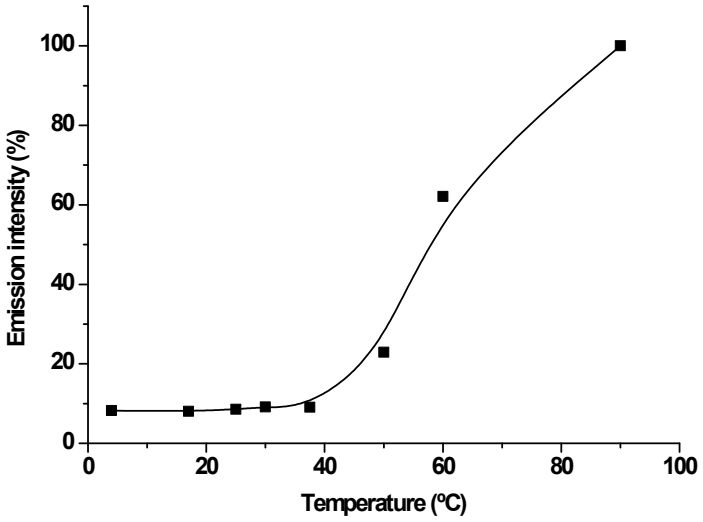

Figure SI-4. Dye release profiles of **S1-P** solid at different temperatures.

Reloading procedure.

Bearing in mind that the transformation from α-helix to random coil is reversible, it occurred to us that **S1-P** could be reloaded and reused. In order to test this appealing possibility solid **S1-P** (2 mg) was suspended in PBS (2 mL) at 90 ºC in order to achieve a nearly complete safranine O release. After 24 hours of stirring (the PBS solution was replaced each 2 hours) the vast majority of the entrapped dye was released. Then the solid was dried under vacuum and suspended again in a 2 ml of concentrated safranine O solution at stirred at 90 ºC during 12 hours. After that, solid was suddenly introduced in an ice bath (in order to assure that **P** is in their α-helix conformation), filtered and again dried. From a safranine O calibration curve and by measuring the absorbance of the solution before and after their contact with solid **S1-P** the quantity of dye reloaded is determined (0.147 g dye / g SiO_2). The reloaded solid was suspended in buffer solution (2 mL) and stirred at 4 ºC during 12 hours (the solid is in their closed state because **P** is in their α-helix conformation). After that, the solid was centrifuged and the safranine O release was determined through UV-visible measurements. Only 4% of the loaded safranine O was released at this temperature. Moreover studies of cargo release at different temperatures displayed a similar profile to that shown in Figure 2.

Circular dichroism (CD) studies

In order to investigate the conformation of peptide **P** in solution, circular dichroisms measurements were carried out. The dichroism spectra in the UV region were obtained in a JASCO 710 circular dichroism spectrometer. The spectra were recorded between 193 and 240 nm using 1 mm optical path cuvettes. The scan speed was fixed at 0.2 nm s^{-1} with an integration time constant of 1 s. The final spectrums were obtained as an average of 20 scans for each sample. The blank spectra were performed in the same conditions as the samples spectra. Solutions of peptide **P** (50 μM) were prepared in 10 mM phosphate buffer at pH 7 with 25 mM NaCl. The concentration of the peptide was determined by UV spectroscopy, using ε_{276} =1460 $M^{-1}cm^{-1}$ for the tyrosine residue.[1] Also 30% TFE were used as a secondary structure stabilizer.[2,3] The spectra were measured at different temperatures starting from the lower until the higher.

Then, the spectra were measured in the inverse gradient to check that the changes in the secondary structure of the peptide were reversible. The temperatures chosen were 4, 15, 30, 45, 60, 75 and 90 ºC waiting at least five minutes between each change in order to equilibrate all the system. The CD spectra in the far UV region of **P** at lower temperatures showed one maxima (at ca. 190 nm) and two minima (centered at ca. 207 and 222 nm) characteristic of peptides adopting an helicoidal conformation (see Figure SI-5).[4] The CD measurements also showed that peptide **P** adopts an α-helix conformation at lower temperatures that changed to a random coil disposition upon heating (see Figure SI-6 for the distribution of α-helix conformation at several temperatures).

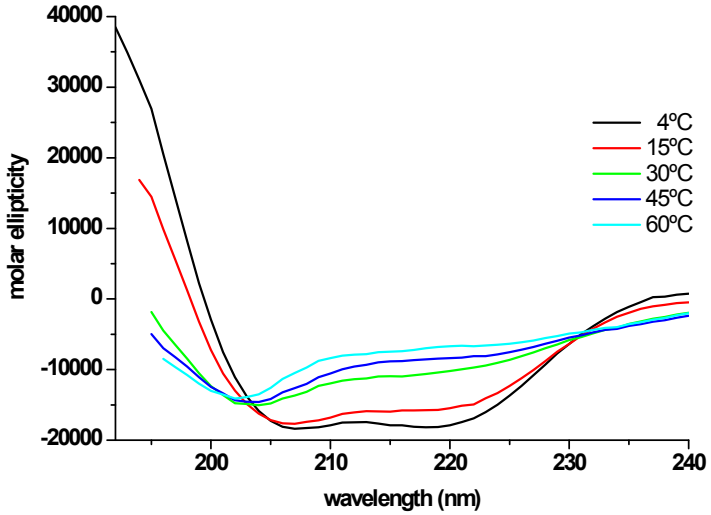

Figure SI-5. CD spectra of 17-mer peptide **P** at different temperatures.

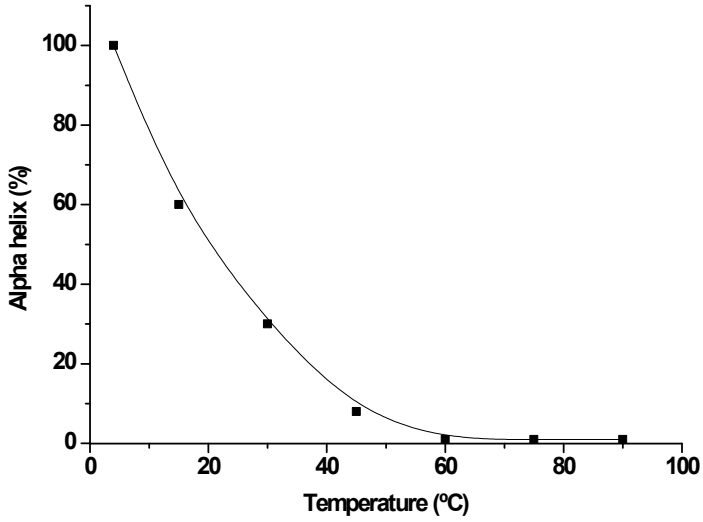

Figure SI-6. CD spectra of 17-mer peptide **P** at different temperatures. The % of α-helix in the peptide was predicted using the AGADIR algorithm.[5]

References

1. S. C. Gill, P. H. von Hippel, *Chem. Biol.* 1989, **182**, 319-326.

2. S. Y. Lau, A. K. Taneja, R. S. Hodges, *J. Biol. Chem.* 1984, **259**, 13253-13261.

3. T. M. Cooper, R. W. Woody, *Biopolymers* 1990, **30**, 657-676.

4. G. Holzwarth, P. Doty, *J. Am. Chem. Soc.* 1965, **87**, 218-228.

5. (a) V. Muñóz, L. Serrano, *Nat. Struct. Mol. Biol.* 1994, **1**, 399-409; (b) V. Muñóz, L. Serrano, *J. Mol. Biol.* 1994, **245**, 275-296; (c) V. Muñóz, L. Serrano, *J. Mol. Biol.* 1994, **245**, 297-308.